Integrative analysis of transcriptomic and metabolomic profiles reveals new insights into the molecular foundation of fruit quality formation in *Citrullus lanatus* (Thunb.) Matsum. & Nakai

Shunpeng Chu (楚顺鹏)[1†], Shuoshuo Wang (王硕硕)[1†], Ruimin Zhang (张锐敏)[1,2], Mengmeng Yin (尹萌萌)[1], Xiaoyu Yang (杨晓玉)[1,2]*, Qinghua Shi (史庆华)[1,2]*

[1] College of Horticulture Science and Engineering, Shandong Agricultural University, Tai'an, Shandong 271018, China;

[2] State Key Laboratory of Crop Biology, Shandong Agricultural University, Tai'an, Shandong 271018, China;

[†]Shunpeng Chu and Shuoshuo Wang are co-first authors.

* Corresponding xiaoyu.yang@sdau.edu.cn and qhshi@sdau.edu.cn

Abstract

In this study, an integrated transcriptome and metabolome analysis was used to explore the molecular foundation of fruit quality in two parent lines of *Citrullus lanatus* with distinct flesh characteristics, including '14-1' (sweet, red, and soft) and 'W600' (bitter, light yellow, and firm), as well as the corresponding F_1 population (bitter, light yellow, and firm). Numerous differentially expressed genes (DEGs) were identified in the fruit samples: 3,766 DEGs for '14-1' vs. 'W600', 2,767 for '14-1' vs. F_1, and 1,178 for F_1 vs. 'W600' at the transition stage; and 4,221 for '14-1' vs. 'W600', 2,447 for '14-1' vs. F_1, and 446 for F_1 vs. 'W600' at the maturity stage. Weighted gene co-expression network analysis (WGCNA) revealed that a gene module including 1,111 DEGs was closely associated with flesh taste and color, and another gene module including 1,575 DEGs contributed significantly to flesh texture. The metabolomic results showed that there were 447 differential metabolites (DMs) for '14-1' vs. 'W600' fruits, 394 for '14-1' vs. F_1, and 298 for F_1 vs. 'W600' at the maturity stage. Combining WGNCA and metabolomic results, several DEGs and DMs were further identified as hub players in fruit quality formation: six DEGs with four DMs for flesh sweetness; six DEGs with 13 DMs for bitterness; nine DEGs with 10 DMs for flesh color; and nine DEGs with four DMs for flesh texture. Altogether, these observations not only expand our knowledge of the molecular basis of fruit quality in watermelon, but also provide potential targets for future watermelon improvement.

Keywords: Fruit Quality; Metabolome; Molecular foundation; Transcriptome; Watermelon

Introduction

Watermelon [*Citrullus lanatus* (Thunb.) Matsum. and Nakai (2n=2x=22)] is a popular fruit crop in the Cucurbitaceae family that is cultivated all over the world, with annual production being highest in China, Turkey, and Iran (Guo *et al*., 2019; Pal *et al*., 2020). It is native to Africa and can be taxonomically divided into seven different species (Ren *et al*., 2017; Guo *et al*., 2019). As an important dietary source, watermelon fruits contain a variety of health-promoting phytochemicals such as sugars, lycopene, and amino acids (Guo *et al*, 2013). Therefore, its fruit quality has attracted extensive attention from horticultural researchers and breeders, and significant effort has been made in elucidating the molecular foundation of quality-related traits such as taste, color, and texture.

Sweetness is closely associated with sugar content in fruits. While sucrose is the most stored sugar in watermelon fruits, oligosaccharides usually serve as the major form of transported sugars from source leaves, along with a small amount of sucrose and hexose followed by a hydrolysis process (Zhang *et al*., 2012). Previous studies have demonstrated that the transport, hydrolysis, and storage courses of sugars from source leaves to fruits are strictly controlled by a series of genetic loci/genes in watermelon, such as *BCE2.1* and *BCE8.1* (Liu *et al*., 2014), *ClTST2* (Ren *et al*., 2017), *ClVST1* (Gao *et al*., 2018a), and *ClAGA1*, *ClSWEET3,* and *ClTST2* (Ren, *et al*., 2021). Using comparative transcriptomic investigation of watermelon fruits with distinct flesh flavors, various differentially expressed genes (DEGs) related to soluble sugar accumulation and metabolism have been identified, providing a genome-wide view of fruit sweetness regulation (Gao *et al*., 2018). A more recent report demonstrated that *ClAGA2*, which encodes an alkaline alpha-galactosidase, can serve as a crucial modulator for the hydrolysis process of stachyose and raffinose in the vascular bundle of watermelon, while sugar transport and storage are controlled by *ClSWEET3* (*C. lanatus Sugars Will Eventually Be Exported Transporter 3*) and *ClTST2* in the plasma membrane and vacuoles of fruit cells, respectively (Ren, *et al*., 2021). In contrast to sweet fruits from cultivated watermelons, progenitor watermelon generally produces small-sized fruits with bitter or bland flesh—a flavor trait that is closely associated with the biosynthesis and accumulation of the cucurbitacin group, particularly cucurbitacin E glycosides, which are Cucurbitaceae plant-specific tetracyclic terpenes with biological significance, including anti-pathogenic effects (Yousaf *et al*., 2018; Kim *et al*., 2020). Regarding the genetic basis for bitterness, several candidate loci/genes have been detected, such as

qbt-c1-1 (Li *et al*., 2018) and *Cla011508* (Gong *et al*., 2022). Furthermore, two acetyltransferases (ACT1/ACT2) and one UDP-glucosyltransferase (UGT) have been revealed to be critical players in the production of cucurbitacin derivatives based on enzymatic assay results (Kim *et al.*, 2020). Using a high-density genetic map constructed via re-sequencing of two watermelon parent lines and a recombinant inbred line (RIL) population, Li *et al*. (2018) successfully mapped one locus (*qbt-c1-1*) responsible for flesh bitterness on chromosome 1, one locus (*qsc-c3-1*) responsible for seed coat color on chromosome 3, and one locus (*qrc-c8-1*) responsible for rind color on chromosome 8 (Li *et al*., 2018).

In addition to sweetness/bitterness, flesh color and firmness are two important sensory quality parameters of watermelon fruits. Previous studies have demonstrated that the differences in the coloration of horticultural products among different species or different accessions can mainly be attributed to the variations in the amounts and categories of carotenoids, which are controlled by different loci/genes related to the biosynthesis and accumulation of carotenoids, such as *LCYB4.1*, *ClPHT4;2*, *ClPSY1*, *ClPAP,* or *ClLCYB* (Liu *et al.*, 2015; Zhang *et al.*, 2016; Fang *et al.*, 2020; Zhang *et al.*, 2020; Guo *et al*.,2021; Xu *et al*., 2021). Based on a transcriptomic investigation of the fruits of five watermelon accessions at different developmental stages, four candidate genes (*Cla003760*, *Cla007686*, *Cla018406,* and *Cla021635*) were found to play essential roles in the coloration of watermelon fruits (Yuan *et al*., 2021). For flesh firmness, a close association has been revealed with cellulose and pectin contents, as well as genes involved in their metabolism (Brummell *et al*., 2004; Qin *et al*.,2007; Sun *et al*., 2020; Anees *et al*., 2021; Chen *et al*.,2021). However, some contradicting observations suggest that fruit firmness exhibits little relationship with cellulose or pectin content in previous studies (Hiwasa *et al*., 2004; Figueroa *et al*., 2010). The involvement of phytohormone signaling and long non-coding RNAs (lncRNAs) has been demonstrated in the regulation of fruit softening/firmness (Lindo-García *et al*., 2019; Chen *et al*., 2021; Li *et al*., 2021).

In the past several years, integrative profiling of the transcriptome and metabolome has been used to explore the regulatory networks underlying fruit quality formation in watermelon. For example, combining RNA sequencing (RNA-seq) and high-performance liquid chromatography (HPLC)-based metabolomic analysis, Umer *et al.* (2020) found that sugars and organic acids were highly correlated with three gene networks/modules in watermelon, including 2,443 genes, of which seven were proposed as critical regulators of the metabolism of sucrose, as well as malic and citric acid (Umer *et*

al.,2020). Similarly, a series of hub genes and metabolites related to flesh taste have been identified based on transcriptomic and metabolomic profiling of wild and cultivated watermelon fruits at different developmental stages (Gong *et al*., 2021). Although great improvements in our mechanistic understanding of fruit quality formation have been obtained at both single gene/locus and genome-wide levels, the complexity and large divergence in the regulation of quality-related traits among different plant materials emphasizes the need to further explore their molecular foundation in watermelon.

In this study, fruit quality was investigated using an integrated transcriptome and metabolome approach for '14-1', 'W600', and F_1 hybrid watermelons, which display apparent variations in flesh taste, color, and texture. A large divergence in both transcriptomic and metabolic profiles was identified among the three samples, providing a comprehensive explanation for their phenotypical variations. A series of hub genes and metabolites closely associated with flesh taste, color, and texture were identified and could be used as potential targets for watermelon improvement in the future.

Materials and Methods

Plant materials

Wild and cultivated watermelon [*Citrullus lanatus* (Thunb.) Matsum. & Nakai] accessions 'W600' and '14-1', which were collected and stored in our laboratory, were used as the male and female parents, respectively, to construct an F_1 hybrid population. After sterilization, 100 watermelon seeds of 'W600', '14-1', or F_1 were grown in plastic pots with nutrient soil and placed in a growth chamber that was set at a 14-h light period with 28°C air temperature, 10-h dark period with 26°C air temperature, and approximately 60% relative humidity. At the three-leaf stage, the seedlings were cultivated in the greenhouse of Shandong Agricultural University, China, from March to June in 2021 with a plant spacing of 40 × 80 cm. Standard field management was carried out during the cultivation period. Two even-sized fruits were collected as one biological repeat at the transition stage [approximately 21 days after pollination (DAP)] and maturity stages (approximately 35 DAP) for phenotypical and multi-omic investigation. Three biological repeats were prepared.

Phenotypical investigation

Flesh hardness was measured with a digital fruit hardness tester with an 8-mm probe (STEP Systems, Germany). Briefly, the sampled fruit was first longitudinally divided into two halves, and the flesh hardness was then determined by vertically inserting the probe into the central flesh of one divided half until the calibration line. The values in the hardness tester were collected and converted into flesh firmness readings according to the manufacturer's instructions. The soluble solid content (SSC) of the central flesh was measured with a PAL-1 digital pocket refractometer (ATAGO, Japan). A total of 16 randomly selected points (eight per fruit) in the central flesh was used for the evaluation of flesh hardness and SSC. After removing values with a large variance, the remaining data were averaged as flesh hardness or SSC for each repeat. Fruit sweetness/bitterness was determined by following the human tasting method previously introduced by Zhang *et al*. (2013). Briefly, participants were randomly selected to taste the fruits from different watermelon inbred lines with a gargling interval between each line, and the tasted fruits were generally classified into bitter and non-bitter groups based on the participants' responses (Mondal *et al.*, 2016; Guo *et al.*, 2019; Santis *et al.*, 2020).

For flesh color, visual observation was adopted according to the protocol previously introduced by Guo *et al*. (2019). All flesh firmness and SSC data were statistically analyzed with SPSS v26 software (IBM Corp., Armonk, NY, USA)

Nanopore RNA sequencing and data analysis

Total RNA extraction from fruit samples, quality evaluation, and library construction were performed according to the standard protocol provided by Oxford Nanopore Technologies. Long-read sequencing was then conducted for the libraries with the Oxford Nanopore PromethION flow cells (FLO-PRO002) in Benagene Company (Wuhan, China). After removal of the low-quality reads using an in-house script, the remaining reads were subjected to identification and classification of full-length transcripts followed by alignment to the watermelon '97103' v2 reference genome (http://cucurbitgenomics.org/organism/21) with the aid of the Pychopper v2.4.0 (-Q 7, -z 50) and Pinfish v0.1.0 packages under default settings, respectively. The abundance of genome-matched transcripts was calculated and normalized as fragments per kilobase transcript per million mapped reads (FPKM). The DEGs were identified in each comparison of transcriptomic samples, with the cutoff parameters of fold-change > 2 and *P*-value < 0.05. Kyoto Encyclopedia of Genes and Genomes

(KEGG) analysis was carried out for the DEGs in R, and the terms with a *P*-value < 0.05 were considered as significantly enriched. For weighted gene co-expression network analysis (WGCNA) analysis, the DEGs were first divided into different modules, and the correlation between DEG FPKMs in each module and flesh quality parameters (SSC, color, and hardness) of the two parents and F_1 plants was then evaluated and displayed in a heatmap using the online BMKCloud Visualization Toolkit (http://en.biocloud.net/toolset).

Sample preparation for metabolome and data analysis

For untargeted gas chromatography-mass spectrometry (GC-MS) analysis of the metabolome, 80 mg of fresh flesh was placed into a 1.5-mL Eppendorf tube with 360 µL precooled methanol and 40 µL 0.3 mg mL^{-1} 2-chloro-L-phenylalanine; the latter used as an internal standard. After being frozen at −20°C for 2 min, the mixture was ground well for 2 min with a JXFSTPRP-24/32 tissue grinder (Jingxin, China) set at a frequency of 60 Hz. The ground flesh was subjected to ultrasonic extraction at 4°C for 30 min followed by the addition of 200 µL chloroform and 400 µL MilliQ H_2O, followed by a second round of 30-min ultrasonic extraction at 4°C. The resulting sample was frozen at −20°C for 30 min and centrifuged at 13,000 rpm for 10 min at 4°C. Two hundred microliters of supernatant was transferred to a glass sampling vial for vacuum-drying at room temperature, and the dried sample was resuspended in 80 µL of 15 mg mL^{-1} methoxylamine hydrochloride solution followed by 2 min of vigorous vortexing and 90 min of incubation at 37°C. After the addition of 80 µL of BSTFA derivatization reagent [containing 1% (v/v) trimethylchlorosilane (TMCS)] and 20 µL n-hexane, the resuspension was vigorously vortexed for 2 min, derivatized at 70°C for 60 min, and finally subjected to GC-MS analysis according to a previous protocol (Yan *et al*., 2020).

To perform untargeted liquid chromatography-mass spectrometry (LC-MS) analysis of the metabolome, 80 mg flesh sample was placed into a 1.5-mL Eppendorf tube with 1 mL 70% (v/v) methanol and 20 µL 0.3 mg mL^{-1} 2-chloro-L-phenylalanine; the latter used as an internal standard. The mixture was kept at −20°C for 2 min and then homogenized for 2 min with the abovementioned tissue grinder at 60 Hz. After 30 min ultrasonic extraction at 4°C, the resulting sample was kept at −20°C overnight and centrifuged at 13,000 rpm at 4°C for 10 min. The supernatant (150 µL) was transferred to an LC vial through a 0.22-µm syringe filter for subsequent LC-MS investigation.

For targeted metabolomic analysis, 50 mg of freeze-dried and pulverized flesh sample was treated with 500 µL extraction buffer, which was composed of 0.01% (w/v) BHT in a solution of n-hexane, acetone, and ethanol (1:1:1, v/v/v). Additionally, 10 µL 20 µg mL^{-1} 2-chloro-L-phenylalanine was added as an internal control. The resulting mixture was vortexed for 20 min at room temperature and subjected to 5-min centrifugation at 4°C. The supernatant was transferred to a brown vial, and the pellet was re-extracted by following the abovementioned protocol. Both supernatants were pooled together, evaporation-dried under nitrogen gas, and resuspended in the mixture of methanol and MTBE at a volume ratio of 1:1. The resuspension was filtered into a LC vial through a 0.22-µm syringe filter for ultra-performance (UP)LC-MS investigation.

The raw data of the untargeted and targeted metabolomes were analyzed with Progenesis QI v2.3 (https://www.nonlinear.com/) and MultiQuant v3.0.3 software (https://sciex.com/products/), respectively. The overall distribution and reproducibility of the metabolome data from all fruit samples were then evaluated by following the principal component analysis (PCA) protocol as described previously (Worley *et al*., 2013). Differential metabolites (DMs) in each comparison of fruit samples were identified with the cutoff parameters of VIP (variable importance in the projection) > 1 and *P*-value < 0.05 for untargeted metabolome datasets, and fold-change > 2 and *P*-value < 0.05 for the targeted metabolome datasets.

Quantitative real time (qRT)-PCR verification

For experimental verification of the DEGs, total RNAs were extracted from fruit samples following a previously reported method (Yang *et al*., 2021). Using 1 µg total RNA as the template, the first-strand cDNAs were synthesized with a RevertAid RT Reverse Transcription Kit (Thermo, USA) following the manufacturer's instructions. Quantitative RT-PCR analyses for selected DEGs were conducted on an ABI 7500 Real-Time PCR System (Applied Biosystems, USA) using the corresponding primers, which were designed using Primer Premier 5.0 software (https://en.freedownloadmanager.org/users-choice/Primer_5.0_Free_Download.html). For each DEG, three biological repeats together with three technical repeats were prepared, and the relative expression was calculated according to the $2^{-\Delta\Delta Ct}$ method as described by Livak and Schmittgen (2001). All qRT-PCR primers have been provided in Table S1.

Statistical analysis

The flesh firmness and SSC data were statistically analyzed using one-way analysis of variance (ANOVA) in SPSS 26.0 at a significance level of 0.05 between each sample. The results were displayed as the mean ± standard deviation of three biological repeats.

High-throughput sequencing data availability

All RNA-seq datasets were deposited in the NCBI Sequence Read Archive database (http://www.ncbi.nlm.nih.gov/sra/) with accession no. PRJNA784391.

Results and discussion

Phenotypic variations in watermelon fruits from two parent lines and F_1 plants

To understand the inheritance of fruit quality-related traits, an F_1 hybrid population was generated from the crossing of watermelon inbred lines '14-1' and 'W600', which were used as the female and male parents, respectively. We focused on flesh taste, color, and texture in the fruits of F_1 plants, because these traits were quite distinct in the two parent lines according to our previous field observations. Phenotypic investigation was carried out for the fruits from two parent lines and F_1 plants at both the transition and maturity stages. The results showed that, at the transition stage, the fruit flesh of 'W600', '14-1', and F_1 was white in color and exhibited no significance differences (Figure 1A). At the maturity stage, while the flesh of '14-1' was red in color, only a slight color change was observed from white to light yellow for the flesh of 'W600' and F_1 (Figure 1A). In terms of flesh texture, significant differences between the three watermelon lines were observed. The fruits of 'W600' were the hardest (21.2 and 16.8 kg cm^{-2}), followed by F_1 (12.1 and 9.1 kg cm^{-2}) and '14-1' (2.4 and 2.3 kg cm^{-2}) at both investigation stages (Figure 1B). A general decreasing trend was also confirmed for flesh hardness with the development of the watermelon fruits (Figure 1B). Being consistent with bitter taste, SSC levels in the flesh at the transition and maturity stages were only 3 and 3.1 for 'W600' and 3.1 and 3.6 for F_1 (Figure 1C). By contrast, the SSC level was significantly increased from 6.1 at the transition stage to 13.4 at the maturity stage in the flesh of '14-1', thus leading to the sweet taste of '14-1' fruits. Dramatic accumulation of sugars at the maturity stage has been observed for watermelon inbred lines with sweet fruits in previous studies (Gao *et al*., 2018;

Ren *et al*., 2021), implying that maturation-related signaling might play a critical role in flesh flavor formation.

Transcriptomic and metabolomic variations in watermelon fruits from the two parent lines and F_1 plants

We initially wondered how these fruit quality-related traits were transcriptionally regulated. To this end, Nanopore sequencing was carried out for RNA samples obtained from '14-1', 'W600', and F_1 fruits at the transition and maturity stages. Three biological repeats were tested for each sample. In contrast to previous studies (Anees *et al*., 2021; Giulia *et al*., 2018), where in two inbred lines with distinct fruit traits have typically been used for RNA-seq analysis, we added the F_1 population together with the two parent lines for transcriptomic comparison to improve the precision of hub gene identification due to increased phenotypic variations. The similar strategy has been adopted by a recent report (Sun *et al*., 2020). After discarding the low-quality reads, over 3,900,000 genome-matched reads were obtained for all libraries, which accounted for over 78% of clean sequenced reads (Table S2). A variable number of full-length unique transcripts were further identified in the fruit samples of '14-1' (10,459–13,706 for the transition stage and 8,598–9,686 for the maturity stage), 'W600' (7,945–14,049 for the transition stage and 6,526–7,995 for the maturity stage), and F_1 (6,692–9,685 for the transition stage and 6,610–8,503 for the maturity stage) (Table S2), covering more than 97% of the annotated genes in the watermelon genome. PCA analysis was carried out for all datasets, and the results indicated that the three biological repeats clustered together for each fruit sample, demonstrating the reproducibility of the Nanopore RNA sequencing libraries. Both high mapping efficiency and good reproducibility evidenced the high quality of the transcriptomic datasets.

A comparison of the transcriptomic profiles was next performed among different fruit samples, and a series of DEGs were identified with the cutoff parameters of fold-change > 2 and *P*-value < 0.05. For '14-1' vs. 'W600', there were 1,804 up-regulated DEGs and 1,962 down-regulated DEGs at the transition stage, as well as 1,975 up-regulated DEGs and 2,246 down-regulated DEGs at the maturity stage; for '14-1' vs. F_1, 1,359 and 1,003 DEGs were upregulated at the transition and maturity stages, respectively, while 1,408 and 1,444 DEGs were downregulated at the transition and maturity stages, respectively. For F_1 vs. 'W600', the number of upregulated DEGs was 675 for the transition stage and 435 for the maturity stage, while the number of downregulated DEGs was 503 for the transition

stage and 281 for the maturity stage (Figure 2A; Table S3). We randomly selected 12 DEGs for qRT-PCR verification using the same RNA samples as for the Nanopore sequencing, and the experimental results were consistent with their FPKM variations in the different fruit samples, further supporting the reliability of our transcriptomic results.

We assessed how these DEGs contributed to phenotypic variations in the fruits of the three watermelon lines. Accordingly, WGCNA—an algorithm used for discovering high correlations between gene clusters/modules to phenotypes of interest (Umer *et al*., 2020)—was adopted to investigate the relationship of the identified DEGs with fruit quality-related parameters, including flesh sweetness/bitterness, color, and hardness. All DEGs that were identified in different sample comparisons were first divided into 12 distinct gene modules of different colors based on their expression patterns, and the correlation efficiency between each gene module and quality parameter was then calculated. The results showed that the darkgreen module composed of 1,111 DEGs displayed a significant correlation with both flesh sweetness (R^2 = 0.97) and color (R^2 = 0.95), and the darkred module that was composed of 1,575 DEGs was significantly associated with flesh bitterness and hardness (R^2 = 0.85) (Figure 2; Table S4). KEGG analysis was performed for DEGs in the darkgreen and darkred modules. A total of five KEGG terms, including “Carotenoid biosynthesis”, “Fatty acid metabolism”, and “Pyruvate metabolism”, were enriched for DEGs in the darkgreen module, and 18 terms such as “Pentose phosphate pathway”, “Plant hormone signal transduction”, and “Lysine biosynthesis” were observed for the DEGs in the darkred module following the cutoff parameter of *P*-value < 0.05 (Table S5).

Metabolomic variations in watermelon fruits from the two parent lines and F_1 plants

Recently, metabolomics has been used to monitor the variations in metabolites at the global level in crop plants upon developmental clues or stressful conditions (Qiu *et al*., 2020), providing a metabolic explanation for their quality formation or acclimation to unfavorable environments. To explore the global variations in metabolite profiles, both untargeted and targeted metabolomic analyses were carried out for the fruit samples of ‘14-1’, ‘W600’, and F_1 at the maturity stage, when apparent differences were observed for quality-related traits including flesh taste, color, and texture among the three watermelon lines. The PCA results showed that three biological repeats for each metabolomic preparation were reproducible (Figure S2), demonstrating that high-quality metabolome datasets were obtained. We further performed metabolite comparison in the different

fruit samples, and the DMs were identified using the cutoff parameters of VIP > 1 and *P*-value < 0.05 for both LC-MS- and GC-MS-based untargeted metabolomes. In the comparison of '14-1' vs. 'W600', the contents of 214 and 199 metabolites were significantly enhanced and reduced, respectively; in the comparison of '14-1' vs. F_1, 204 metabolites displayed dramatically increased contents, while 146 metabolites displayed dramatically decreased contents; and in the comparison of F_1 vs. 'W600', the number of significantly increased metabolites was 124, while the number of significantly decreased metabolites was 148 (Figure 3A and B; Table S6).

Flesh coloration largely depends on watermelon cultivars and carotenoid categories and contents (Guo *et al*., 2019). To explore the molecular mechanisms underlying different flesh colors in the three watermelon samples, targeted metabolomics analysis was employed to monitor metabolite changes in the carotenoid metabolic pathway in 'W600', '14-1', and F_1 mature fruits. The differential carotenoids were identified using the cutoff parameters of fold-change > 2 and *P*-value < 0.05. The number of enhanced carotenoids was 11 for '14-1' vs. 'W600', 13 for '14-1' vs. F_1, and 12 for F_1 vs. 'W600', while the contents of 23, 21, and 16 carotenoids were significantly reduced in the comparisons of '14-1' vs. 'W600', '14-1' vs. F_1, and F_1 vs. 'W600', respectively (Figure 3C). Apparent variations in metabolite profiles have been observed in different cultivars of horticultural crops such as tomato (Bai *et al*., 2021) and melon (Biais *et al*., 2010).

Molecular insights into flesh taste, color, and texture in watermelon

To obtain a comprehensive understanding of fruit quality formation, we analyzed the combined contributions of transcriptomic and metabolomic variations to the phenotypic differences in flesh taste, color, and texture of '14-1', 'W600', and F_1 fruits. Previous studies have demonstrated that the major form of soluble sugars in watermelon fruits is sucrose (Figure 4E), which serves as the determinant for flesh sweetness (Zhu *et al*., 2017; Zamuz *et al*., 2021). Sucrose content in fruits can be influenced by various genes encoding metabolism-related enzymes such as SuSy (Liu *et al*.,2013; Zhu *et al*., 2017) and transporters such as *TST* (Huang *et al*.,2020). In our former WGCNA analysis, a close association of the darkgreen gene module, which was composed of 1,111 DEGs, was revealed with flesh sweetness/bitterness. As the soluble solid content of '14-1' was significantly higher than that of W600 and F_1, and the soluble solid content of W600 and F_1 was constantly at a comparatively low level, we speculated that the major contributors to flesh sweetness might be '14-1'-specific DEGs in the darkgreen gene module (Figure 4A). We identified a total of 323 DEGs of this type,

among which six genes (*Cla97C08G153160*, *Cla97C05G101500*, *Cla97C10G204040*, *Cla97C07G131650*, *Cla97C01G001950,* and *Cla97C04G070460*) have been demonstrated to be involved in the sucrose biosynthesis pathway in previous studies (Figure 4B; Yativ *et al*., 2010; Dai *et al*., 2011).

Interestingly, a recent publication demonstrated that *ClAGA2* (*Cla97C04G070460*), which encodes an alkaline alpha-galactosidase, can serve as a crucial modulator for the hydrolysis process of stachyose and raffinose in the vascular bundle of watermelon, while sugar transport and storage are controlled by *ClSWEET3* and *ClTST2* in the plasma membrane and vacuoles of fruit cells, respectively (Ren, *et al*., 2021). This evidence points to the functional conservation of *Cla97C04G070460* in sucrose metabolism, which could be used as a potential target locus for the flesh taste improvement of watermelon fruits.

The metabolites in the sucrose biosynthesis pathway were further investigated, and the contents of sucrose, D-fructose-6-phosphate, glucose-1-phosphate, and inulobiose were observed to be overrepresented in '14-1' flesh in comparison to that of 'W600' and F_1 (Figure 4B). These observations largely corroborate the report of Liu *et al.* (2013), wherein the sucrose content in sweet watermelon was significantly higher than in non-sweet watermelon. In addition, sucrose content in watermelon fruits can also be influenced by developmental stages and cultivation conditions (Meng *et al*., 2009; Liu *et al*., 2013). To analyze the association between DEGs and sucrose metabolism, a correlation analysis was carried out between the six DEGs and four metabolites, and the highest correlation was observed for *Cla97C08G153160* and inulobiose (R^2 = 0.9999), followed by *Cla97C01G001950* and glucose-1-phosphate (R^2 = 0.9992) and *Cla97C07G131650* and sucrose (R^2 = 0.9973) (Figure 4C).

In contrast to the sweet flesh of '14-1', the fruits of 'W600' and F_1 possessed an apparent bitter taste, which is mainly caused by the accumulation of cucurbitacin E glycosides (Guo *et al*., 2019). Using a high-density genetic map constructed via re-sequencing of two watermelon parent lines and a RIL population, Li *et al*. (2018) successfully mapped one locus (*qbt-c1-1*) responsible for flesh bitterness on chromosome 1 (Li *et al*., 2018). To explore the potential genes closely associated with cucurbitacin metabolism, we focused on the darkred gene module and found that 406 DEGs displayed a 'W600' and F_1-specific distribution (Figure 5A). Based the annotation information, six

genes (*Cla97C09G173590*, *Cla97C11G210690*, *Cla97C05G101010*, *Cla97C01G003790*, *Cla97C05G100930,* and *Cla97C05G100990*) out of the 406 DEGs were proposed to be directly involved in flesh bitterness regulation in watermelon (Figure 5B). Cucurbitacin biosynthesis mainly includes terpenoid skeleton formation and oxidative modifications, and the modification reactions are commonly controlled by *ACTs* (acetyltransferases), *CYP450s* (*cytochrome P450s*), and *OSCs* (*oxidosqualene cyclases*) (Zhou *et al*., 2016; Kim *et al*., 2020). The OSC gene family is highly conserved in the plant kingdom, and the critical roles of different *OSC*s have been revealed in the catalyzation of terpenoid skeletons to generate specific cucurbitacin (Thimmappa *et al*., 2014). By contrast, we observed that four *CYP450* genes (*Cla97C05G101010*, *Cla97C01G003790*, *Cla97C05G100930*, and *Cla97C05G100990*), the expression of which was apparently higher in 'W600' than in '14-1', were closely related to cucurbitacin E biosynthesis (Zhou *et al*., 2016), perhaps reflecting a distinct regulatory network for bitterness formation in 'W600' fruits. It should be noted that *Cla97C09G173590*, which encodes a geranylgeranyl pyrophosphate synthase and functions as a rate-limiting factor in the synthesis pathway of cucurbitacins (Chen *et al*., 2005), was classified as a '14-1'-specfic DEG in the darkred gene module, but its abundance was constantly higher in the flesh of 'W600' and F_1 in comparison to that of '14-1' (Table S6), providing a reasonable explanation for the differences in flesh flavor among the three watermelon lines. Variable proportions and categories of cucurbitacins have been reported in different watermelon varieties (Lavie *et al*., 1964), leading to distinct flesh flavors. We further explored the metabolites in the cucurbitacin biosynthesis pathway, and the content of cucurbitacin E (Figure 5E) was over-accumulated in 'W600' and F_1 flesh in comparison to that of '14-1' (Figure 5C). The contributions of cucurbitacin-related DEGs to DMs were evaluated, and a high correlation was observed for *Cla97C09G173590* and absinthin (R^2 = 0.9989), cucurbitacin I 2-glucoside (R^2 = 0.9989), and cucurbitacin F (R^2 = 0.9971), while *Cla97C05G100990* displayed the lowest correlation with L-tyrosine (Figure 5C). The manner in which *Cla97C09G173590* is involved in the regulation of flesh taste deserves further exploration in the future.

Flesh color is largely dependent on the composition and contents of carotenoids, and can thus be regulated by genes involved in carotenoid metabolism (Zhao *et al*., 2013). Based on the WGCNA analysis, we found that DEGs in the darkgreen gene module were significantly related to flesh color (Figure 6A). Based on the observation of a striking color change from white to red for '14-1' flesh, but only a slight color change for 'W600' and F_1 flesh, at the two investigation stages, it might be proposed that the DEGs closely associated with flesh coloration might be '14-1'-specific. We

identified a total of 323 '14-1'-specfic DEGs, which included various key genes in the carotenoid metabolic pathway, such as PSY and NCED, in the darkgreen gene module (Figure 2D). Using an F2:3 population, Sandra *et al*. (2017) mapped a major QTL related to watermelon flesh color and further discovered that *Cla97C01G008760* encoding a PSY is the candidate gene, the expression of which was positively correlated with the accumulation of lycopene. Lycopene is the main form of carotenoid that is responsible for the red flesh of a major proportion of cultivated watermelons (Figure 6D; Liu *et al*., 2012). By contrast, yellow flesh is mainly attributed to the accumulation of violanthin and lutein in watermelon, while the depletion of carotenoids leads to white flesh, a typical trait for fruits of wild watermelon (Hermanns *et al*., 2020). Using targeted metabolomic analysis, a total of 36 metabolites were identified, of which 10 (γ-carotene, β-carotene, lycopene, (E/Z)-phytoene, α-cryptoxanthin, β-cryptoxanthin, lutein, neoxanthin, violaxanthin, and zeaxanthin) were directly derived from the carotenoid metabolic pathway and displayed differential accumulation in the fruit flesh between '14-1' and the other two lines (Figure 6C), providing a metabolic explanation for the large divergence in flesh color among the three watermelon lines. A correlation analysis was further carried out between the carotenoid-related DEGs and metabolites. The correlation coefficients between the seven DMs (γ-carotene, β-carotene, lycopene, (E/Z)-phytoene, α-cryptoxanthin, β-cryptoxanthin, and zeaxanthin) and DEGs were all greater than 0.9, while a weak correlation was observed between the other three DMs (violaxanthin, neoxanthin, and lutein) and the DEGs (Figure 6B). This observation was consistent with the previous claim that flesh color might be genetically controlled by a complex regulatory network (Zhao *et al*., 2013, Wang *et al*., 2019; Hermanns *et al*., 2020).

Flesh hardness, a quality trait genetically controlled by QTLs, has been demonstrated to be determined to a great extent by the contents of cell-wall components such as cellulose and pectin (Sun *et al*., 2020). Bulked segregant analysis (BSA) has demonstrated that *Cla016033* and *Cla012507* can influence flesh hardness by regulating cell wall composition and fruit maturity (Sun *et al*., 2020). In a study carried out by Sehgal *et al.* (2021), *Cla012351* encoding a cellulose synthase and *Cla004251* encoding a pectinesterase were observed to be key players in the metabolism of cellulose and pectin due to their high correlation with the contents of cellulose and pectin in watermelon fruits. Our phenotypic results showed that '14-1' yielded fruits with soft flesh, and the degree of its flesh firmness was almost constant at both the transition and maturity stages, while for 'W600' and F_1, both firm flesh and significantly varied hardness were observed at the two investigation points, indicating that hardness-related DEGs might be 'W600'/F_1-specific. We identified a total of 406

'W600'/F_1-specific DEGs in the darkred gene module, which displayed a close association with flesh hardness in the WGCNA analysis. Interestingly, nine genes (*Cla97C09G163490*, *Cla97C03G065030*, *Cla97C06G110120*, *Cla97C05G098130*, *Cla97C05G108640*, *Cla97C04G070440*, *Cla97C08G146150*, *Cla97C01G019430,* and *Cla97C06G118820*) of the 'W600'/F_1-specific DEGs might function as critical players in cellulose and pectin degradation according to their annotation information (Figure 7A and C). Liao *et al*. (2020) reported a high correlation between ethylene responsive transcription factor 4 (*ERF4*) and the firmness of watermelon peel, partially supporting that *Cla97C06G118820* encoding an ERF might be profoundly involved in the regulation of flesh firmness. To provide functional evidence for these DEGs, the contents of cellulose and pectin-related metabolites were further explored in an untargeted metabolomic analysis, and four DMs were identified, including galactonic acid, pectin, ethyl cellulose, and D-galactose (Figure 7B; Table S3). As a main component of the cell wall, pectin can be divided into protopectin, soluble pectin, and pectin acid, and the degradation of protopectin to soluble pectin leads to fruit softening (Figueroa *et al*., 2010). Correlation investigation was further carried out between the firmness-related DEGs and DMs, and the highest correlation with pectin was observed for *Cla97C09G163490* (R^2 = 0.9821) followed by *Cla97C04G070440* (R^2 = 0.9773) (Figure 7), while the poorest correlation was revealed between *Cla97C05G108640* and ethyl cellulose (Figure 7B).

Conclusion

In the present study, an integrated transcriptome and metabolome approach was adopted to investigate the molecular foundation of flesh taste, color, and texture in the fruits of '14-1', 'W600', and F_1 hybrid lines. Significant divergence was revealed in both the transcriptomic and metabolomic profiles of the fruits from the three watermelon lines, providing a comprehensive explanation for their phenotypic variations. A series of hub genes and metabolites closely associated with flesh taste, color, and texture were identified and could be used as potential targets for watermelon improvement in the future.

Author Contributions

Qinghua Shi and Xiaoyu Yang conceived the research; Shunpeng Chu and Mengmeng Yin performed the experiments; Shunpeng Chu, Shuoshuo Wang, Qinghua Shi and Xiaoyu Yang analyzed data; Qinghua Shi, Xiaoyu Yang, Shunpeng Chu, Shuoshuo Wang wrote the manuscript; Ruimin Zhang provided technical assistance during manuscript preparation. All authors read and approved the final manuscript.

Funding

This work was supported by Agricultural Variety Improvement Project of Shandong Province (2019LZGC005) and Shandong Vegetable Research System (SDAIT-05).

Conflict of Interest

The authors declare no conflict of interest.

References

Anees, M., Gao, L., Umer, M. J., *et al*. (2021). Identification of key gene networks associated with cell wall components leading to flesh firmness in watermelon. *Frontiers in Plant Science*, 12: 630243.

Bai, C. M., Wu, C. E., Ma, L. L., *et al*. (2021). Transcriptomics and metabolomics analyses provide insights into postharvest ripening and senescence of tomato fruit under low temperature. *Horticultural Plant Journal*. doi. org/10.1016/j.hpj.2021.09.001

Biais, B., Beauvoit, B., Allwood, J. W., *et al*. (2010). Metabolic acclimation to hypoxia revealed by metabolite gradients in melon fruit. *Journal of Plant Physiology*, 167: 242-245.

Brummell, D. A., Dal Cin, V., Crisosto, C. H., *et al*. (2004). Cell wall metabolism during maturation, ripening and senescence of peach fruit. *Journal of Experimental Botany*, 55: 2029-2039.

Cai, Y. E., Fang, X. F., He, C. W., *et al*. (2015). Cucurbitacins: a systematic review of the phytochemistry and anticancer activity. *The American Journal of Chinese Medicine*, 43: 1331-1350.

Chen, Y. T., Cheng, C. Z., Feng, X., *et al*. (2021). Integrated analysis of lncRNA and mRNA transcriptomes reveals the potential regulatory role of lncRNA in kiwifruit ripening and softening. *Scientific Reports*, 11: 1671.

Chen, J. C., Chiu, M. H., Nie, R. L., *et al*. (2005). Cucurbitacins and cucurbitane glycosides: structures and biological activities. *Cheminform*, 22: 386-399.

Dai, N., Cohen, S., Portnoy, V., *et al*. (2011). Metabolism of soluble sugars in developing melon fruit: a global transcriptional view of the metabolic transition to sucrose accumulation. *Plant Molecular Biology*, 76: 1-18.

Fang, X. F., Liu, S., Gao, P., *et al*. (2020). Expression of *ClPAP* and *ClPSY1* in watermelon correlates with chromoplast differentiation, carotenoid accumulation, and flesh color formation. *Scientia Horticulturae*, 270: 109437.

Figueroa, C. R., Rosli, H. G., Civello, P. M., *et al*. (2010). Changes in cell wall polysaccharides and cell wall degrading enzymes during ripening of *Fragaria chiloensis* and *Fragaria × ananassa fruits*. *Scientia Horticulturae*, 124: 454-462.

Giulia, B., Anna, R., Maurizio, G., *et al*. (2018). External maturity indicators, carotenoid and sugar compositions and volatile patterns in 'Cuoredolce ; ' and 'Rugby' mini-watermelon (*Citrullus lanatus* (Thunb) Matsumura & Nakai) varieties in relation of ripening degree at harvest. *Postharvest Biology & Technology*, 136:1-11.

Gao, L., Zhao, S. J., Lu, X. Q., *et al*. (2018). Comparative transcriptome analysis reveals key genes potentially related to soluble sugar and organic acid accumulation in watermelon. *Plos One*, 13: e0190096.

Gong, C. S., Li, B. B., Anees, M., *et al*. (2022). Fine-mapping reveals that the bHLH gene *Cla011508* regulates the bitterness of watermelon fruit. *Scientia Horticulturae*, 292: 110626.

Gong, C. S., Zhu, H. J., Lu, X. Q., *et al*. (2021). An integrated transcriptome and metabolome approach reveals the accumulation of taste-related metabolites and gene regulatory networks during watermelon fruit development. *Planta*, 254: 35.

Guo, S. G., Zhang, J. G., Sun, H. H., *et al*. (2013). The draft genome of watermelon (*Citrullus lanatus*) and resequencing of 20 diverse accessions. *Nature Genetics*, 45: 51-58.

Guo, S. G., Zhao, S. J., Sun, H. H., *et al*. (2019). Resequencing of 414 cultivated and wild watermelon accessions identifies selection for fruit quality traits. *Nature Genetics*, 51: 1616-1623.

Guo, Y. M., Bai, J. J., Duan, X. D., *et al*. (2021). Accumulation characteristics of carotenoids and adaptive fruit color variation in ornamental pepper. *Scientia Horticulturae*, 275: 109699.

Huang, W. F., Hu, B., Liu, J. L., *et al*. (2020). Identification and characterization of tonoplast sugar transporter (TST) gene family in cucumber. *Horticultural Plant Journal*, 6: 145-157.

Hermanns, A. S., Zhou, X. S., Xu, Q., *et al*. (2020). Carotenoid pigment accumulation in horticultural plants. *Horticultural Plant Journal*, 6: 343-360.

Hiwasa, K., Nakano, R., Hashimoto, A., *et al*. (2004). European, Chinese and Japanese pear fruits exhibit differential softening characteristics during ripening. *Journal of Experimental Botany*, 55: 2281-90.

Jing, S. Y., Zou, H. Y., Wu, Z. D., *et al*. (2020). Cucurbitacins: bioactivities and synergistic effect with small-molecule drugs. *Journal of Functional Foods*, 72: 104042.

Kim, Y., Choi, D., Zhang, C. Y., *et al*. (2018). Profiling cucurbitacins from diverse watermelons (*Citrullus spp*.). *Horticulture, Environment, and Biotechnology*, 59: 557-566.

Kim, Y. C., Choi, D., Cha. A., *et al*. (2020). Critical enzymes for biosynthesis of cucurbitacin derivatives in watermelon and their biological significance. *Communications Biology*, 3: 444.

Ko, H., Ho, L., Neuhaus, H. E., *et al*. (2021). Transporter SlSWEET15 unloads sucrose from phloem and seed coat for fruit and seed development in tomato. *Plant Physiology*, 00: 1-16.

Kang, B. S., Zhao, W. E., Hou, Y. B., *et al*. (2010). Expression of carotenogenic genes during the development and ripening of watermelon fruit. *Scientia Horticulturae*, 124:368-375.

Li, B. B., Lu, X. Q., Dou, J. L., *et al*. (2018). Construction of a high-density genetic map and mapping of fruit traits in watermelon (*Citrullus Lanatus* L.) based on whole-genome resequencing. *International Journal of Molecular Sciences*, 19: 3268.

Li, S., Chen, K. S., Grierson, D. (2021). Molecular and hormonal mechanisms regulating fleshy fruit ripening. *Cells*, 10: 1136.

Lindo-García, V., Muoz, P., Larrigaudière, C., *et al*. (2019). Interplay between hormones and assimilates during pear development and ripening and its relationship with the fruit postharvest behaviour. *Plant Science*, 291: 110339.

Liu, S., Gao, P., Wang, X. Z., *et al*., (2014). Mapping of quantitative trait loci for lycopene content and fruit traits in *Citrullus lanatus*. *Euphytica*, 202: 411-426.

Liu, C. H., Zhang, H. Y., Dai, Z. Y., *et al*. (2012). Volatile chemical and carotenoid profiles in watermelons [*Citrullus vulgaris* (Thunb.) Schrad (Cucurbitaceae)] with different flesh colors. *Food Science and Biotechnology*, 21: 531-541.

Liu, J. A., Guo, S. G., He, H. J., *et al*. (2013). Dynamic characteristics of sugar accumulation and related enzyme activities in sweet and non-sweet watermelon fruits. *Acta Physiologiae Plantarum*, 35: 3213-3222.

Liu, S., Gao, P., Wang, X. Z., et al. (2015). Mapping of quantitative trait loci for lycopene content and fruit traits in *Citrullus lanatus*. *Euphytica*, 202: 411-426.

Livak, K. J., Schmittgen, T. D. (2001). Analysis of relative gene expression data using real-time quantitative PCR and the $2^{-\Delta\Delta Ct}$ method. *Methods*, 25: 402-408.

Lu, M. Z., Snyder, R., Grant, J., *et al*. (2020). Manipulation of sucrose phloem and embryo loading affects pea leaf metabolism, carbon and nitrogen partitioning to sinks as well as seed storage pools. *The Plant Journal*, 101: 217-236.

Lavie, D., Willner, D., Merenlender, Z. (1964). Constituents of Citrullus colocynthis (L.) Schrad. *Phytochemistry*, 3:51-56.

Mondal, A., Saxena D. (2016). Development of barley grass juice and wheat grass juice as functional food with added other fruit juices and their organoleptic evaluation.

Pal, S., Rao, E.S., Sriram, S. (2020). Genetic analysis of resistance to *Fusarium oxysporum* f. sp. *niveum* race 2 in cultivated watermelon [*Citrullus lanatus* (Thunb.) Matsum & Nakai]. *Australasian Plant Pathol*, 49: 319-326.

Qin, L., Ren, X. L. (2007). Characteristics of texture change with Qinguan and Fuji apples during ripening. *Molecules*, 16: 213-216.

Qiu, W. W., Su, W. Q., Cai, Z. Y., *et al*. (2020). Combined analysis of transcriptome and metabolome reveals the potential mechanism of coloration and fruit quality in yellow and purple *Passiflora edulis* Sims. *Journal of Agricultural and Food Chemistry*, 68: 12096-12106.

Ren, Y., Guo, S. G., Zhang, J., *et al*. (2017). A tonoplast sugar transporter underlies a sugar accumulation QTL in watermelon. *Plant Physiology*, 176: 836-850.

Ren, Y., Li, M. Y., Guo, S. G., *et al*. (2021). Evolutionary gain of oligosaccharide hydrolysis and sugar transport enhanced carbohydrate partitioning in sweet watermelon fruits. *The Plant Cell*, 0: 1-20.

Sandra., Branham., Lea., *et al*. (2017). Genetic mapping of a major codominant QTL associated with β-carotene accumulation in watermelon. *Molecular Breeding*, 37:146-146.

Salehi, B., Quispe, C., Sharifi-Rad, J., *et al*. (2021). Antioxidant potential of family Cucurbitaceae with special emphasis on *Cucurbita genus*: a key to alleviate oxidative stress-mediated disorders. *Phytotherapy Research*, 35: 1-25.

Sehgal, D., Quraishi, U. M., AnEeS, M., *et al*. (2021). Identification of Key Gene Networks Associated With Cell Wall Components Leading to Flesh Firmness in Watermelon. *Frontiers in Plant Science*, 12.

Santis, D. D., Frangipane M T. (2020). Citrus aurantium L.: Cultivar impact on sensory profile. *International Journal of Gastronomy and Food Science*, 20.

Sun, L., Zhang, Y. S., Cui, H. N., *et al*. (2020). Linkage mapping and comparative transcriptome analysis of firmness in watermelon (*Citrullus lanatus*). *Frontiers in Plant Science*, 11: 831.

Thimmappa, R., Geisler, K., Louveau, T., *et al*. (2014). Triterpene biosynthesis in plants. *Annual Review of Plant Biology*, 65:225-257.

Umer, M. J., Safdar, L. B., Gebremeskel, H., *et al.* (2020). Identification of key gene networks controlling organic acid and sugar metabolism during watermelon fruit development by integrating metabolic phenotypes and gene expression profiles. *Horticulture Research*, 7: 193.

Wang, C. N., Qiao, A. H., Fang, X. F., *et al*. (2019). Fine mapping of lycopene content and flesh color related gene and development of molecular marker-assisted selection for flesh color in watermelon (*Citrullus lanatus*). *Frontiers in Plant Science*, 10: 1240.

Worley, B., Powers, R., (2013). Multivariate analysis in metabolomics. *Current Metabolomics*, 1: 92-107.

Meng, W. H., Zhang, X., Luo, T., *et al*. (2009). Influences of rootstocks on the sugar accumulation and activities of sucrose metabolism related enzymes in Citrullus lanatus by grafting. *Journal of Northwest A & F University*(Natural Science Edition), 127-132.

Xu, X. Y., Lu, X. N., Tang, Z., *et al*. (2021). Combined analysis of carotenoid metabolites and the transcriptome to reveal the molecular mechanism underlying fruit colouration in zucchini (*Cucurbita pepo* L.). *Food Chemistry: Molecular Sciences*, 2: 100021.

Yativ, M., Harary, I., Wolf, S. (2010). Sucrose accumulation in watermelon fruits: genetic variation and biochemical analysis. *Journal of Plant Physiology*, 167: 589-596.

Yan, L., Li, P. Y., Zhao, X. P., *et al*. (2020). Physiological and metabolic responses of maize (Zea mays) plants to Fe3O4 nanoparticles. *Science of The Total Environment*, 718:137400.

Yang, X. Y., You, C. J., Wang, X. F., *et al*. (2021). Widespread occurrence of microRNA-mediated target cleavage on membrane-bound polysomes. *Genome Biology*, 22: 15.`

Yousaf, H. K., Shan, K., Chen, X. W., *et al*. (2018). Impact of the secondary plant metabolite cucurbitacin B on the demographical traits of the melon aphid, *Aphis gossypii*. *Scientific Reports*, 8: 16473.

Yuan, P. L., Umer, M. J., He, N., *et al*. (2021). Transcriptome regulation of carotenoids in five flesh-colored watermelons (*Citrullus lanatus*). *BMC Plant Biology*, 21: 23.

Zamuz, S., Munekata, P. E., Gullón, B., *et al*. (2021). *Citrullus lanatus* as source of bioactive components: an up-to-date review. *Trends in Food Science & Technology*, 111: 208-222.

Zhao, W. E., Lv, P., Gu, H. H. (2013). Studies on carotenoids in watermelon flesh. *Agricultural Sciences*, 4: 13-20.

Zhang, C. K., Yu, X. Y., Ayre, B. G., *et al*. (2012). The origin and composition of cucurbit "Phloem" Exudate. *Plant Physiology*, 158: 1873-1882.

Zhang, J., Guo, S. G., Ren, Y., *et al*. (2016). High-level expression of a novel chromoplast phosphate transporter ClPHT4;2 is required for flesh color development in watermelon. *New Phytologist*, 213: 3.

Zhang, S. P., Miao, H., Sun, R. F., *et al*. (2013). Localization of a new gene for bitterness in cucumber. *Journal of Heredity*, 104: 134-139.

Zhang, J., Sun, H. H., Guo, S. G., *et al*. (2020). Decreased protein abundance of lycopene β-cyclase contributes to red flesh in domesticated watermelon. *Plant Physiology*, 183: 1171-1183.

Zhu, Q. L., Gao, P., Liu, S., *et al*. (2017). Comparative transcriptome analysis of two contrasting watermelon genotypes during fruit development and ripening. *BMC Genomics*, 18: 3.

Zhou, Y., Ma, Y. S., Zeng, J. G., *et al*. (2016). Convergence and divergence of bitterness biosynthesis and regulation in Cucurbitaceae. *Nature Plants*, 2:16183.

Figure legends

Figure 1. Fruit phenotypes of two watermelon parent lines and F_1 plants. (A) Transverse view for watermelon fruits of 'W600', '14-1' and F_1 at the transition and maturity stages. (B-C) Flesh firmness (B) and soluble solid content (SSC, C) for watermelon fruits of 'W600', '14-1' and F_1 at the transition and maturity stages. Data display as mean ± standard deviation of three biological repeats. Different letters indicate significant differences at a statistical level of 0.05 (one-way ANOVA test). TW600, 'W600' fruits at the transition stage; 'T14-1', '14-1' fruits at the transition stage; TF_1, F_1 fruits at the transition stage; MW600, 'W600' fruit at the maturity stage; M14-1, '14-1' fruit at the maturity stage; MF_1, F_1 fruits at the maturity stage.

Figure 2. Transcriptomic variations in the fruits of two watermelon parent lines and F_1 plants. (A) The number of differentially expressed genes (DEGs) in different comparisons of fruit samples. (B) A dendrogram showing gene modules from the weighted gene co-expression network analysis(WGCNA) of DEGs. (C) An optimized dendrogram showing gene modules from the WGCNA analysis of DEGs. (D) A heatmap displaying the correlation between DEG modules and three flesh traits including firmness, color and taste for 'W600', '14-1' and F_1 watermelons. TW600, 'W600' fruits at the transition stage; 'T14-1', '14-1' fruits at the transition stage; TF_1, F_1 fruits at the transition stage; MW600, 'W600' fruit at the maturity stage; M14-1, '14-1' fruit at the maturity stage; MF_1, F_1 fruits at the maturity stage.

Figure 3. Metabolomic variations in the fruits of two watermelon parent lines and F_1 plants. (A-C) Heatmaps showing the identified differential metabolites (DMs) in the fruits of 'MW600', 'M14-1' and MF_1 at the maturity stage by gas chromatography-mass spectrometry (GC-MS, A), liquid chromatograph mass spectrometer (LC-MS, B) and ultra performance liquid chromatography (UPLC, C). MW600, 'W600' fruit at the maturity stage; M14-1, '14-1' fruit at the maturity stage; MF_1, F_1 fruits at the maturity stage.

Figure 4. Correlation analysis of sweetness-related differentially expressed genes (DEGs) and differential metabolites (DMs) in the fruits of two watermelon parent lines and F_1 plants. (A) Venn diagrams showing the distribution of sweetness-related DEGs among 'W600', '14-1' and F_1 fruits.

Top panel: up-regulated DEGs; bottom panel: down-regulated DEGs. (B) A heatmap displaying the abundance of sweetness-related DEGs in the fruits of 'W600', '14-1' and F_1 at the transition and maturity stages. (C) Sugar accumulation in sucrose metabolic pathways in the fruits of 'W600', '14-1' and F_1 at the maturity stage. (D) Correlation of the sweetness-related hub DEGs and DMs in watermelon fruits. (E) MS/MS diagram for sucrose in watermelon fruits. SPS, Sucrose-phosphate synthase; SS, Sucrose synthase. AMY, Alpha-amylase; BGLU, beta-glucosidase; UXS1, UDP-glucuronic acid decarboxylase 1; UXS5, UDP-glucuronic acid decarboxylase 5; TRE, Trehalase; ATSIP, Alkaline alpha-galactosidase seed imbibition protein; TW600: 'W600' fruits at the transition stage; 'T14-1', '14-1' fruits at the transition stage; TF_1, F_1 fruits at the transition stage; MW600, 'W600' fruit at the maturity stage; M14-1, '14-1' fruit at the maturity stage; MF_1, F_1 fruits at the maturity stage.

Figure 5. Correlation analysis of bitterness-related differentially expressed genes (DEGs) and differential metabolites (DMs) in the fruits of two watermelon parent lines and F1 plants. (A) Venn diagrams showing the distribution of bitterness-related DEGs among 'W600', '14-1' and F_1 fruits. Top panel: up-regulated DEGs; bottom panel: down-regulated DEGs. (B) A heatmap displaying the abundance of bitterness-related DEGs in the fruits of 'W600', '14-1' and F_1 at the transition and maturity stages. (C) Contents of bitterness-related DMs in related metabolic pathway in the fruits of 'W600', '14-1' and F_1 at the maturity stages (D) Correlation of the bitterness-related hub DEGs and DMs in watermelon fruits. (E) MS diagram for cucurbitacin E in watermelon fruits. GGPPS, Geranylgeranyl pyrophosphate synthase; CYP, Cytochrome P450; IDI, Isopentenyl diphoshate; GPS, Geranylgeranyl pyrophosphate synthase; FPS, farnesyl pyrophosphate synthase; SQS, Squalene Synthase; SQE, Squalene; OSC, Oxidosqualene cyclase; P450, Cytochrome P450. TW600: 'W600' fruits at the transition stage; 'T14-1', '14-1' fruits at the transition stage; TF_1, F_1 fruits at the transition stage; MW600, 'W600' fruit at the maturity stage; M14-1, '14-1' fruit at the maturity stage; MF_1, F_1 fruits at the maturity stage.

Figure 6. Correlation analysis of coloration-related differentially expressed genes (DEGs) and differential metabolites (DMs) in the fruits of two watermelon parent lines and F_1 plants. (A) A heatmap displaying the expression of carotenoid-related genes in the fruits of 'W600', '14-1' and F_1 at the transition and maturity stages. (B) Contents of coloration-related DMs in carotenoid biosynthetic pathway in the fruits of 'W600', '14-1' and F_1 at the maturity stages. (C) Correlation of the coloration-related hub DEGs and DMs in watermelon fruits. (D) TIC diagrams for lycopene in the

fruits of ‘W600’, ‘14-1’ and F1. CYP, Cytochrome P450; AIR12, Cytochrome b561 and domon domain-containing protein; PSY, phytoene synthase; PDS, phytoene desaturase; Z-ISO, ζ- carotene isomerase; ZDS, ζ-carotene desaturase; LCY, lycopene β-cyclase; ZEP, zeaxanthin epoxidase; VED, violaxanthin de-epoxidase; NXS, neoxanthin synthase; NCED, 9- cis-epoxycarotenoid dioxygenase; CrtISO, carotenoid isomerase; BCH, β-carotene hydroxylase; CYP97A, cytochrome P450 carotene β-hydroxylase; CYP97C, cytochrome P450 carotene ε-hydroxylase. The peak time of lycopene was 8.23 min. TW600: ‘W600’ fruits at the transition stage; T14-1, ‘14-1’ fruits at the transition stage; TF_1, F_1 fruits at the transition stage; MW600, ‘W600’ fruit at the maturity stage; M14-1, ‘14-1’ fruit at the maturity stage; MF_1, F_1 fruits at the maturity stage.

Figure 7. Correlation analysis of hardness-related differentially expressed genes (DEGs) and differential metabolites (DMs) in the fruits of two watermelon parent lines and F_1 plants. (A) A heatmap displaying the expression of hardness-related DEGs in the fruits of ‘W600’, ‘14-1’ and F_1 at the transition and maturity stages. (B) Correlation of the hardness-related hub DEGs and DMs in watermelon fruits. (C) MS/MS diagram for pectin in watermelon fruits. PME inhibitor, pectin methylesterase inhibitor; CESA1, Cellulose synthase 1; CESA2, Cellulose synthase 2; CESA3, Cellulose synthase; CSLC5, Cellulose synthase-like C5; BGAL3, Beta-galactosidase 3; ERF041, Ethylene-responsive transcription factor 1; PME2, Pectinesterase 2; TW600: ‘W600’ fruits at the transition stage; T14-1, ‘14-1’ fruits at the transition stage; TF_1, F_1 fruits at the transition stage; MW600, ‘W600’ fruit at the maturity stage; M14-1, ’14-1’ fruit at the maturity stage; MF_1, F_1 fruits at the maturity stage.

Figure 1

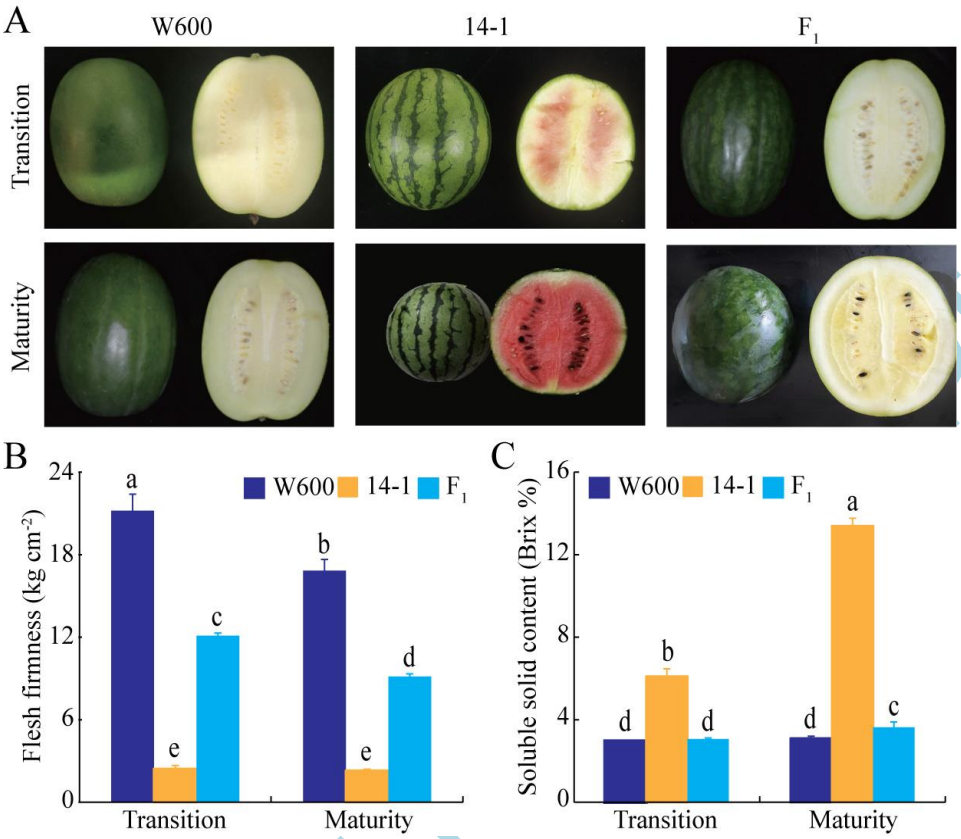

Figure 2

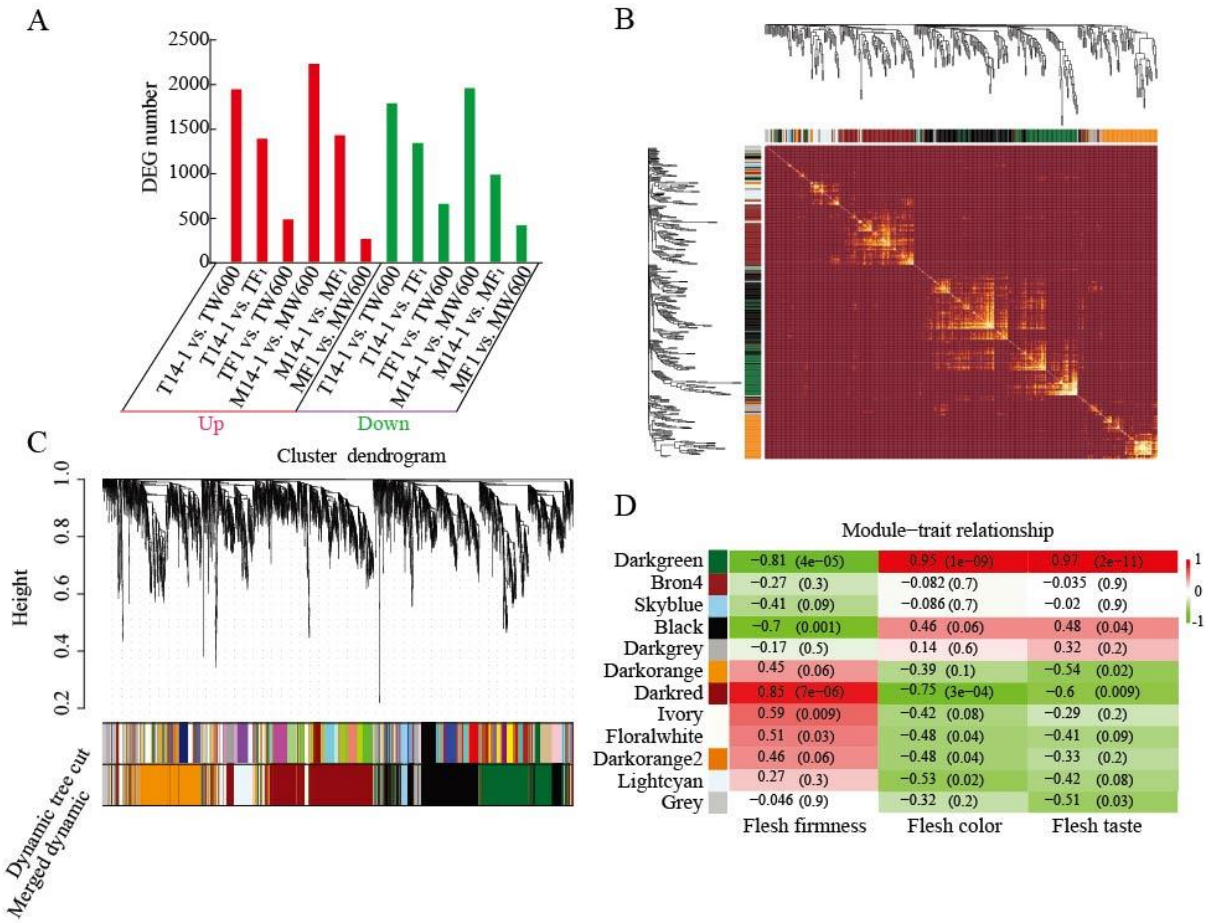

Figure 3

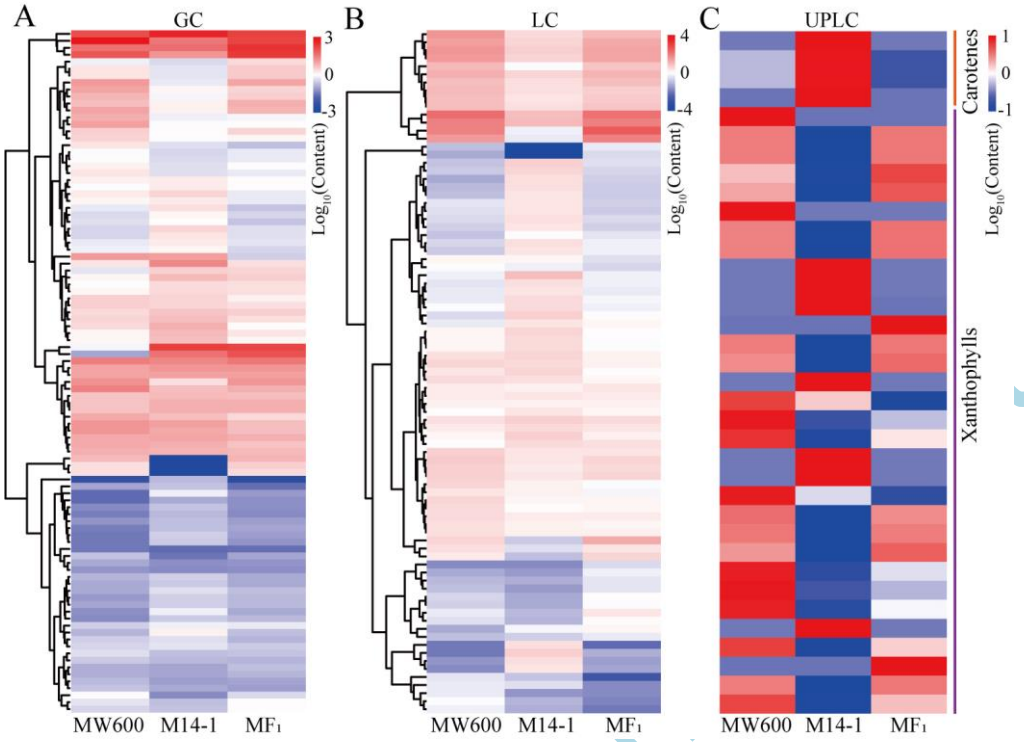

Figure 4

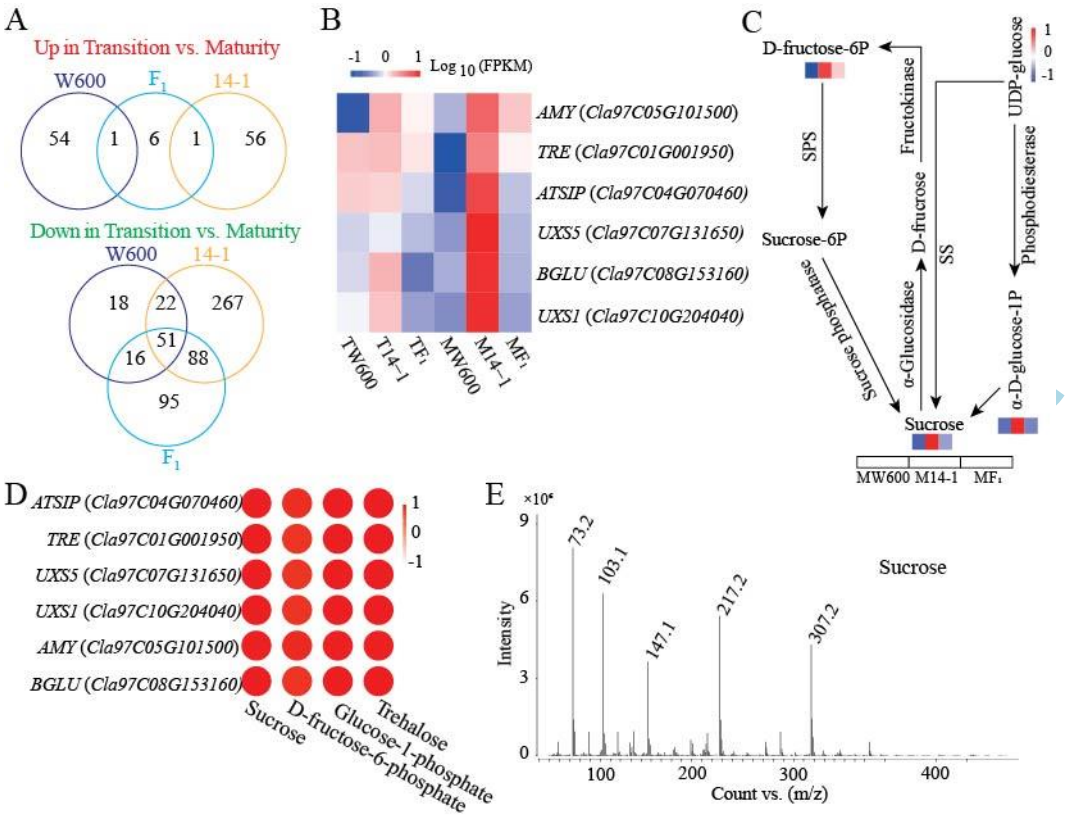

Figure 5

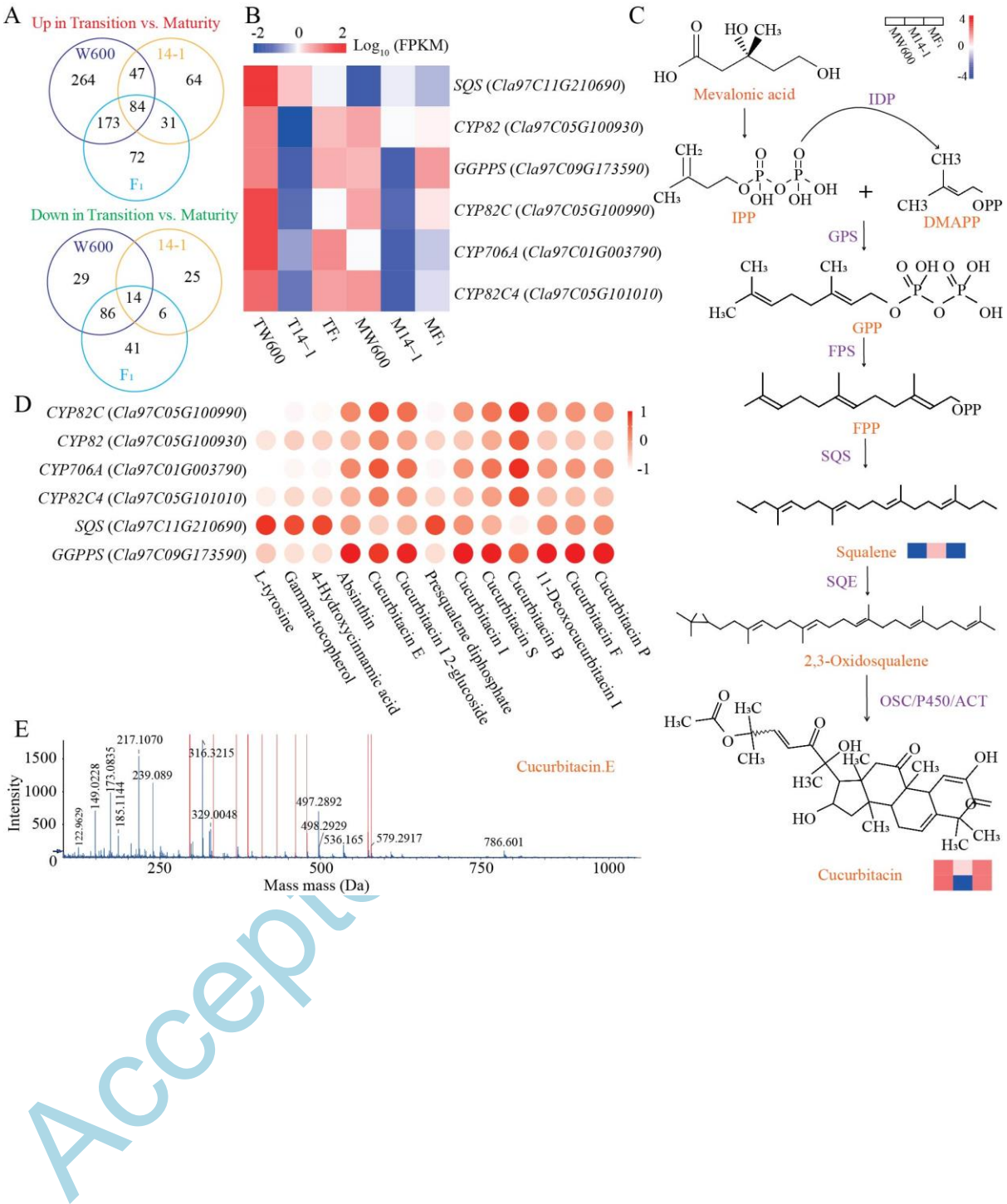

Figure 6

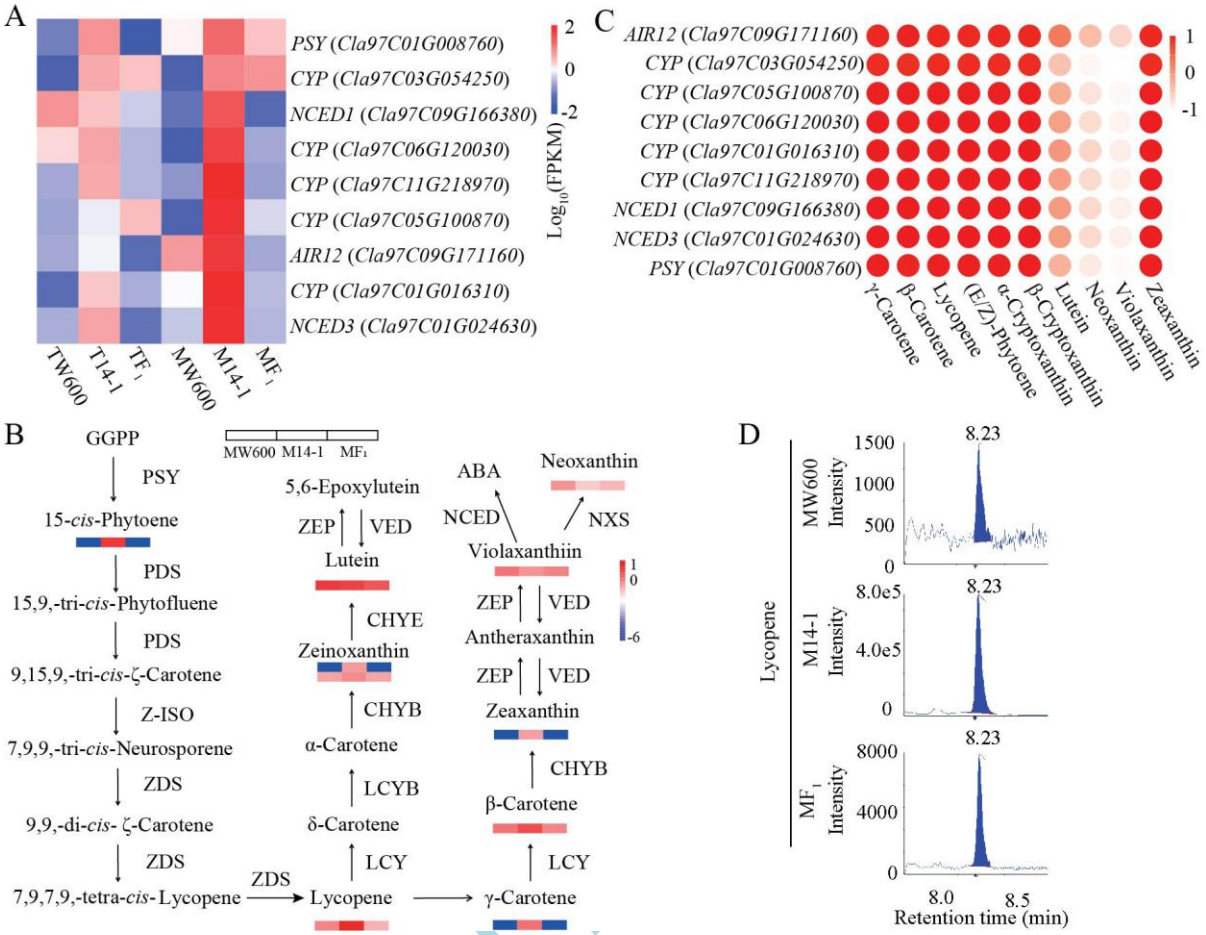

Figure 7